

# The wavelet-aided methods for evaluating the output signal that is designated for uninterruptible power supply systems

**Abstract.** In the article an analysis of the quality of the output voltage for Uninterruptible Power Supply (UPS) was performed. The currently used and commonly known methods for calculating the different quality factors mainly focus on averaging the values of the waveform e.g. Total Harmonic Distortion (THD), Total Distortion Factor (TDF), Weighted Total Harmonic Distortion (WTHD). The main goal of the paper is to propose a complete and supplementary methodology for assessing the quality and parameters that are the complements of the algorithms that are currently used.

**Streszczenie.** W artykule przedstawiono analizę jakości napięcia wyjściowego falowników w systemach bezprzerwowego zasilania UPS. Obecnie znane i stosowane metody wyliczania różnych współczynników skupiają się głównie na wartościach uśrednionych przebiegu wyjściowego. Na przykład są to współczynnik zniekształceń harmoniczných THD, TDF oraz ważony WTHD. Głównym celem artykułu jest przedstawienie kompletnej i dodatkowej procedury pozwalającej na obiektywną ocenę sygnału wyjściowego będącą wsparciem dla stosowanych już metod. (Metody oparte na transformacji falkowej wspomagające ocenę sygnału wyjściowego przeznaczone do modułów bezprzerwowego zasilania UPS.)

**Keywords:** continuous wavelet transform, voltage source inverters, power electronics system, (uninterruptible power supply) UPS.

**Słowa kluczowe:** ciągła transformata falkowa, falowniki napięcia, układy elektroniki mocy, (systemy bezprzerwowego zasilania) UPS.

## Introduction

Methods for evaluating of output voltage are used in many cases, for example in single-phase Voltage Source Inverters (VSI) [1], three-phase VSI [2] with unbalance load [3-4], VSI for motors [5-7] for VSI dedicated to renewable energy sources [8], with different algorithm control [9-12] for VSI with additional boost converters [13] and many more cases. The evaluation of the output voltage quality is related to many aspects, designing, software, and hardware. Analyzing the quality of the output voltage, we can identify the disadvantages of new solutions in power electronics like [14]. Quality of the output voltage is also dependent on the selecting of appropriate components [15-16], attention to the principles of PCB design [17-18], H-bridge control system [19], using multi-level VSI [20-22] and many more conditions.

VSI's are the basic subassembly of Uninterruptible Power Supplies (UPS). Their design process is restricted by the standards related to the power supply systems for static, dynamic linear and nonlinear loads. One of the quality classifiers of the VSI should be an appointment of the deviation from the output AC sinusoidal wave in comparison to the ideal pure sine wave. The acceptable levels of the output voltage distortions are restricted by the standards:

- a) IEEE-519-1992 [23];
- b) EN-62040-3 [24] (together with the IEC-61000-2-2).

The standards also defines the coefficients that describe the quality of the output voltage, mainly Total Harmonic Distortion (THD) and Total Distortion Factor (TDF), acceptable time to steady-state and overshoot possible for different types of loads (static resistive, nonlinear rectified RC and dynamic).

In reference to the fact that a system should be tested under the three types of loads that are presented in Fig. 1, the followed method was used. Taking into account both the changes that are an effect of the changes in the step load and the distortions that are caused by a nonlinear rectified RC load, a reasonable solution seems to be to analyse the output signal by matching signal samples with different characteristics (scale, frequency, shape) to the ideal output the sine wave. The proposed solution uses a wavelet transformation. The main goal of this paper is to describe the methodology of evaluating the common quality coefficient, which permits for the objective evaluation of the VSI output voltage and the quantity of distortions.

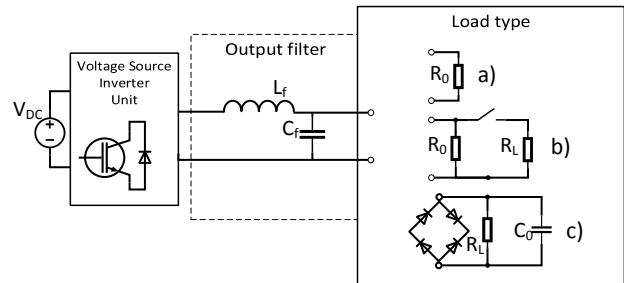


Fig. 1. Typical loads type for the exemplary UPS system.

(a) Static resistive load, (b) Dynamic load – changes between the high and low values of resistance and c) Nonlinear resistive-capacitive load.

## Wavelet background

A wavelet is a function that is described by the following dependency (1):

$$(1) \quad \Psi_{jk} = 2^{j/2} \Psi(2^j t - k)$$

Where  $j$  and  $k$  are integer numbers and the function  $\Psi_{jk}$  (mother wavelet) is an orthonormal base in the Hilbert space. The Hilbert space means the complete inner product. Complete in the significance that every Cauchy sequence of points in metric space  $M$  has a limit in that metric [25]. Based on the definition of a wavelet function, we can adopt a wavelet transform for a continuous signal (2):

$$(2) \quad s_{\Psi}(a, b) = \frac{1}{\sqrt{a}} \int_{-\infty}^{\infty} s(t) \Psi\left(\frac{t-b}{a}\right) dt$$

The continuous wavelet is, therefore, a transform of the signal  $s(t)$  is an element of collection  $L^2$  of the projections onto the analysing function or wavelet [26], where:  $a$  – scale parameter shift in the frequency domain,  $b$  – shift parameter in the time domain  $t$ ,  $s(t)$  – the analyzed signal,  $\Psi((t-b)/a)$  – the wavelet transformation kernel and  $S_{\Psi}(a, b)$  – the wavelet transform. The parameters  $a$  and  $b$  are also commonly called the dilation and translation parameters. They change in a continuous manner. The main application of the wavelet transform is to analyse non-stationary signals, which have changeable means and variances. In these cases, an analysis in the time-frequency domain is required.

Its algorithm is very similar to the commonly used Fourier transform. The key difference depends on the fact that the Fourier transform for a kernel transformation uses sinusoidal functions, while the wavelet transform uses different wavelets kernel. We have the influence on the shape of the mother wavelet that we want to use. Moreover, it is possible to see how long the distortions are for specific frequencies. In order to meet the necessary conditions simultaneously [26-27], the wavelets should be orthogonal, the total mean of the wavelets should be zero and the wavelet functions should have a finite frequency response. The wavelet function  $\Psi(t)$  is an acceptable fundamental wavelet if the admissibility condition is fulfilled (3):

$$(3) \quad C_{\Psi} = \int_0^{\infty} \frac{|\Psi(\omega)|^2}{\omega} d\omega < \infty$$

where  $\Psi(\omega)$  – the Fourier transform of the function  $\Psi(t)$  and  $\omega$  – frequency. Additionally, it is described analytically if (4):

$$(4) \quad \Psi(\omega) = 0 \text{ for } \omega < 0$$

According to the definition, a fundamental wavelet behaves like a bandpass filter. In addition to the fundamental wavelet, we are able to generate a family of wavelets that have different scales and shifts in time. The result of such a wavelet transform are the output coefficients, which define the similarity between the signal and the selected wavelet [26-28]. The results are printed on a scalogram graph in order to present the data as a 3D graph.

#### Selecting the mother wavelet

During the investigations, different wavelet base functions were considered. For the different wavelets with an increasing carrier wave, more oscillations fit into the Gaussian window. A good choice for this application is the analytic wavelet, which is the Morse wavelet (a subsume of the Gaussian and Cauchy wavelets) [26]. The second reason for using this type of wavelet is that it has the flattest Continuous Wavelet Transform (CWT) surface for the ideal sine wave, which is the signal that is generated for the lowest scale. The simulations were performed using the MATLAB CWT function. The formulae for the Morse frequency-domain form (5):

$$(5) \quad \Psi_{\beta,\gamma}(\omega) = U(\omega) \alpha_{\beta,\gamma} \omega^{\beta} e^{-(\omega)^{\gamma}}$$

Where  $U(\omega)$  is the Heaviside step function,  $\alpha_{\beta,\gamma}$  is the normalising constant,  $\beta$  is the amplitude of the wavelet bandpass filter and  $\gamma$  is the symmetry parameter.

#### About the quality parameters

The most commonly used factor for checking the quality is the *THD* factor, which indicates how closely the pulse width modulated voltage follows its sinusoidal reference and it is independent of the frequency. The other commonly used factor is the *Weighted Total Harmonic Distortion (WTHD)*, which is also based on the sum of all squared harmonics, but in addition, considers the order of the harmonics. The higher the order of the harmonics, the lower their influence on the *WTHD* factor is. The main purpose of the experiment was to derive calculations that were not based on the averaging methods – the *Wavelet Factor (WF)*. Although changes in a signal have different causes, it is very important that the overshooting amplitude, which occurs in an enormous way in step load changes, is very dangerous for the endurance of a system.

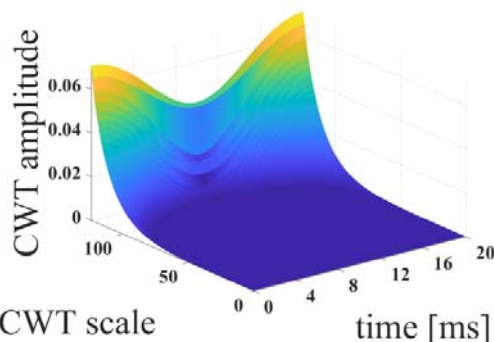
The proposed parameter is based on the area under the curves with reference to the undistorted signal calculation after the CWT transformation. In the calculations, we took into account the first harmonic  $h_1$ . The proposed parameter is very sensitive to all of the changes in the signal curve. In opposite to the different averaging based methods, we were also to find in an easy way the discontinuities as far as the changes connected with the nonlinear rectified RC load.

#### Calculating the wavelet parameters

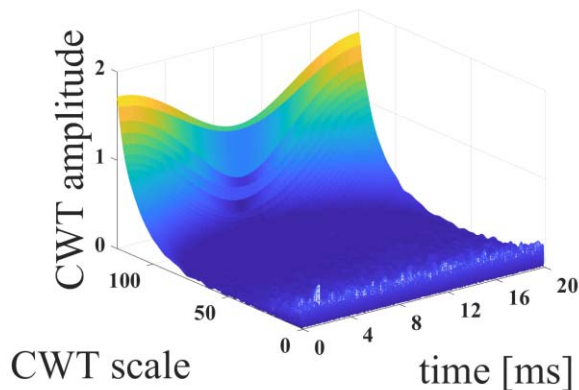
The method that was used in the experiment should start by collecting the waveform points for a specific frequency. During the investigation, the switching frequency in the circuit was  $f_c = 25600$  Hz. The data origin from the experimental single-phase VSI with the STM32 F407VG discovery board included with the different load types. Next, the continuous wavelet transformations for the waveforms for different load types were performed. A matrix of the size  $a \times b$  was the result of each CWT transformation, where  $a$  is the number that indicated the wavelet scale (the higher the scale, the higher the frequency that it refers to). On the other hand,  $b$  is the number of the collected waveform points. The components of the matrix are the complex coefficient values, which was the consequence of using the Morse wavelet. For each scale in each row of the matrix, the absolute value was calculated, during which the volume under the curve of the time-frequency domain output waveform was obtained. Afterward, the ratio of the volume, the maximal scale and number of points were determined. Thus, the proposed WF parameter is (6):

$$(6) \quad WF = \frac{V_1}{V_2}$$

where,  $V_1$  – the volume under the whole curve and  $V_2$  – the volume under the curve in reference to the first harmonic  $h_1$ . The proposed WF factor is dimensionless, which means that it is based on the scale coefficients, which have no units. The value that is calculated is required for the further calculations.



a)



b)

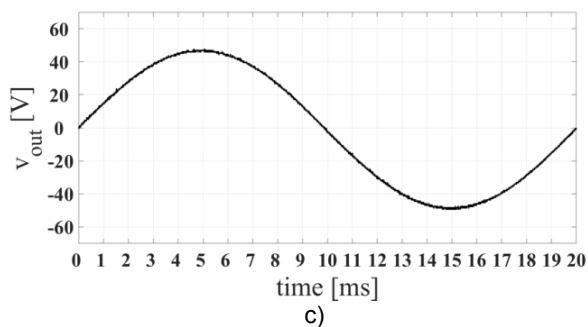


Fig.. 2 Results for the  $R=2000 \Omega$  load. (a) CWT transformation of the signal in reference to the  $h1$ , (b) CWT transformation of the whole measured signal, (c) R load waveform.

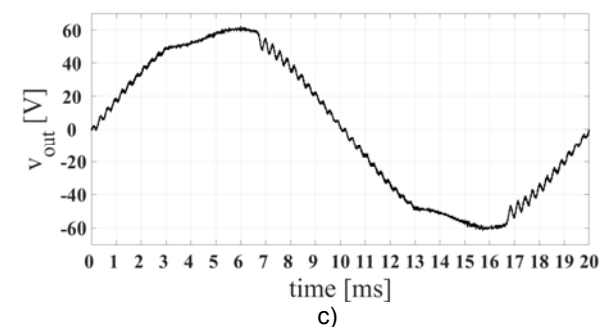
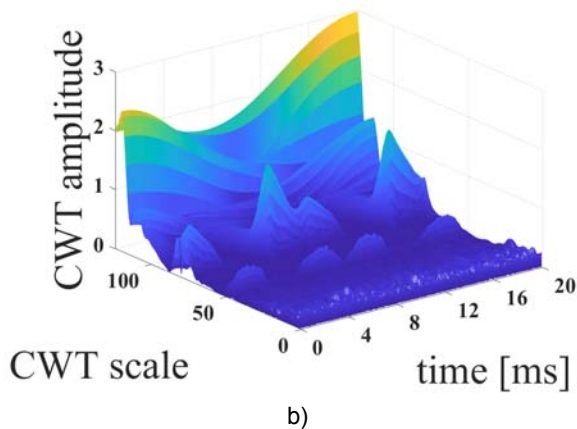
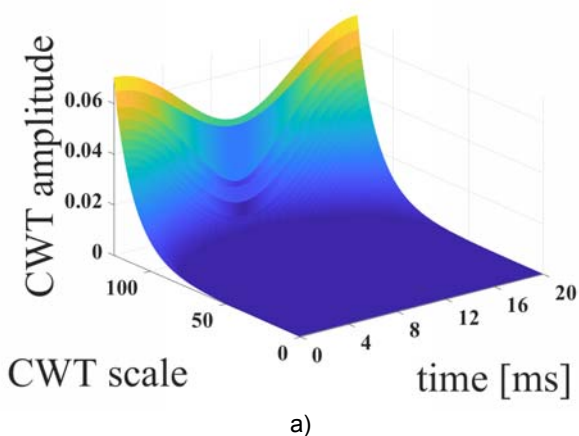
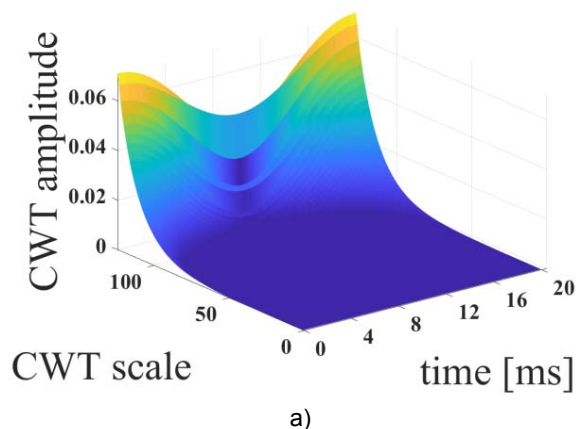


Fig.. 3 Results for the RC load,  $R=100 \Omega$ ,  $C=430 \mu\text{F}$ . (a) CWT transformation of the signal in reference to the  $h1$ , (b) CWT transformation of the whole measured signal, (c) RC load waveform.

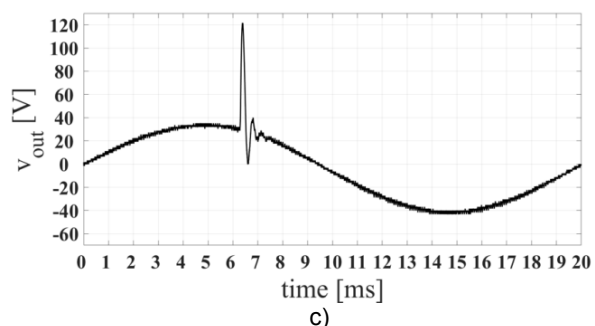
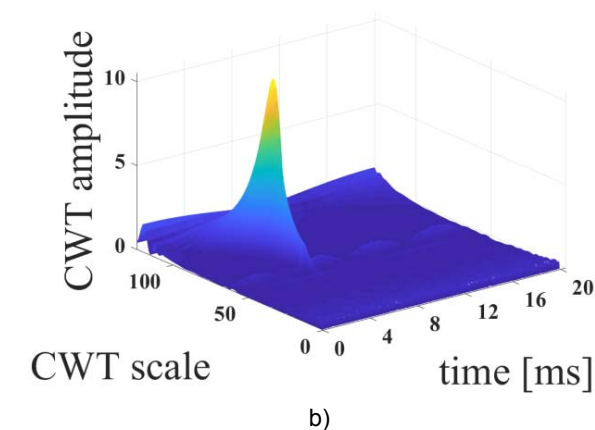


Fig.. 4 Results for the step load change,  $R=45\Omega/R=500\Omega$ . (a) CWT transformation of the signal in reference to the  $h1$ , (b) CWT transformation of the whole measured signal, (c) step load waveform.

### Experimental results

For all of the wavelets that were used in the CWT in MATLAB, the amplitude of the wavelet bandpass filter at the peak frequency for each scale was set to two. Moreover, the default  $\gamma$  symmetry parameter was set to three – the default MATLAB parameter. In order to emphasize the number and types of different distortions, there was no special feedback in the circuit, which is visible in Figs. (2-4). CWT amplitude is the absolute value of CWT coefficient on a specific scale in the time.

### Detecting the high-peak value oscillations

For UPS systems, the short time peak changes during the step load changes are the most dangerous. They are clearly visible when the load that is being used is relieved in VSI. The standard EN 62040:3 [24] covers two parameters for step load changes: the overshoot and the settling time.

As can be observed from Fig. 2 and Fig. 4, the amount of the proposed *WF* factor is relatively high compared to Fig. 3. In order to distinguish the short peaks that are caused by a step load change, the difference between the highest peak and the highest peak in the last wavelet scale was calculated. The Quality Wavelet Factor (*QWF*) should be calculated using the formulae (7):

$$(7) \quad QWF = \left( 1 + \frac{P_a - P_s}{P_s} \right) * WF$$

where:  $P_a$  – the amplitude of the highest peak value in the CWT,  
 $P_s$  – the highest amplitude value in the last scale row in the CWT for the specific load type,  
*QWF* – the proposed quality wavelet factor.

Table 1. Comparison of the output voltage quality factors.

Coefficient	<i>QWF</i>	<i>THD</i>	<i>WTHD</i>
R load	31.97	1.42%	0.35%
RC load	59.47	5.79%	26.51%
Step load-relief	719.53	26.51%	6.17%

As can be observed in Table 1, the *QWF* perfectly maps the quantity of the different distortions that occur in a system. The double-digit representation of the proposed factor indicates a high peak or a significant oscillation in the long-term duration.

### Discussion

The results of the investigations imply that the Continuous Wavelet Transformation together with the proper selection of mother wavelets is one of the solutions of indicating the quality of the output voltage. That simplifies the rating procedure of the output signal. The proposed method could be also checked with different types of converters topologies and shapes of output distortion signal (using, for example, different mother wavelet function). In further research, the Hilbert-Huang and Wigner-Ville transformation could be also compared in the meaning of speed and accuracy in the disturbance location both in time and frequency domain. The properties of signals such as frequency, noisiness, periodicity and predictability of distortion should be taken into account.

### Conclusions

The obtained results qualify the signal regardless of the load type that is selected. The method does not average the signal values. It is also not such sensitive to the number of the probes in comparison to the other well-known FFT-based methods. It can indicate the distortions that are connected with the control with either the load type or the noises that are during the measurements. With the graphical interpretations of the CWT, the *QWF* factor enlarges the presentation of the peaks.

*Funding: This research was funded by the Polish Ministry of Science and Higher Education partially by Statutory Research and partially by Young Researchers funds of Department of Electronics, Electrical Engineering and Microelectronics, Faculty of Automatic Control, Electronics and Computer Science, Silesian University of Technology, Gliwice, Poland. Authors were partially supported by the Polish National Centre for Research and Development, grant no. TANGO3/427467/NCBR/2019.*

*Acknowledgments: The calculations were carried out using the IT infrastructure that was funded by the GeCONiI project (POIG.02.03.01-24-099/13).*

*Authors: mgr inż. Łukasz Dyga, E-mail: lukasz.dyga@polsl.pl; dr hab. inż. Zbigniew Rymarski, prof. Pol. Śl., E-mail: zbigniew.rymarski@polsl.pl; dr inż. Krzysztof Bernacki, E-mail: krzysztof.bernacki@polsl.pl Katedra Elektroniki, Elektrotechniki i Mikroelektroniki, Wydział Automatyki, Elektroniki i Informatyki, ul. Akademicka 16, 44-100 Gliwice.*

### REFERENCES

- [1] Rymarski, Z., Bernacki, K., Dyga, Ł. Some Aspects of Voltage Source Inverter Control. *Elektronika ir Elektrotechnika*, 2017, 23, 26-30. DOI: 10.5755/j01.eie.23.2.17995
- [2] Jun, E., Park, S., Kwak, S. A Comprehensive Double-Vector Approach to Alleviate Common-Mode Voltage in Three-Phase Voltage-Source Inverters with a Predictive Control Algorithm. *Electronics*, 2019, 8, 872. DOI: 10.3390/electronics8080872
- [3] Rymarski, Z., Bernacki, K., Dyga, Ł. A control for an unbalanced 3-phase load in UPS systems. *Elektronika ir Elektrotechnika*, 2018, 24, 27-31. DOI: 10.5755/j01.eie.24.4.21474
- [4] Hintz, A., Prasanna, U., Rajashekara K. Comparative Study of the Three-Phase Grid-Connected Inverter Sharing Unbalanced Three-Phase and/or Single-Phase systems. *IEEE Transaction on Industry Applications*, 2016, 52, 5156-5164. DOI: 10.1109/TIA.2016.2593680
- [5] Srndovic, M., Fiser, R., Grandi G. Analysis of Equivalent Inductance of Three-Phase Induction Motors in the Switching Frequency Range. *Electronics*, 2019, 8, 120. DOI: 10.3390/electronics8020120.
- [6] Rudnicki, T., Sikora, A., Czerwinski, R., Polok, D. Impact of PWM control frequency on efficiency of drive with 1 kW permanent magnet synchronous motor. *Elektronika ir Elektrotechnika*, 2016, 22, 10-16. DOI: 10.5755/j01.eie.22.6.17216.
- [7] Kumar, R., Singh, B. Grid Interactive Solar PV-Based Water Pumping Using BLDC Motor Drive. *IEEE Transaction on Industry Applications*, 2019, 55, 5153-5165. DOI: 10.1109/TIA.2019.2928286
- [8] Khawia, E., Chariag, D., Sbita, L. A Control Strategy for a Three-Phase Grid Connected PV System under Grid Faults. *Electronics*, 2019, 8, 906. DOI: 10.3390/electronics8080906
- [9] Jun, E., Park, S., Kwak, S. Model Predictive Current Control Method with Improved Performances for Three-Phase Voltage Source Inverters. *Electronics*, 2019, 8, 625. DOI: 10.3390/electronics8060625
- [10] Rasool, M., Khan, M., Ahmed, Z., Saeed, M. Analysis of an H<sup>∞</sup> Robust Control for a Three-Phase Voltage Source Inverter. *Inventions*, 2019, 4, 18. DOI: 10.3390/inventions4010018
- [11] Arab, N., Vahedi, H., Al-Haddad K. LQR Control of Single-Phase Grid-Tied PUC5 Inverter With LCL Filter. *IEEE Transaction on Industrial Electronics*, 2019, 67, 297-307. DOI: 10.1109/TIE.2019.2897544
- [12] Rymarski, Z., Bernacki, K., Dyga, Ł., Davari P. Passivity-Based Control Design Methodology for UPS Systems. *Energies*, 2019, 12, 4301, DOI: 10.3390/en1222430
- [13] Rymarski, Z., Bernacki, K., Dyga, Ł. Decreasing the single phase inverter output voltage distortions caused by impedance networks. *IEEE Transaction on Industry Applications*, 2019, 55, pp.7586-7594, DOI:10.1109/TIA.2019.2935418
- [14] Rymarski, Z., Bernacki, K. Drawbacks of impedance networks. *International Journal of Circuit Theory and Applications*, 2018, 46, 612-628. DOI: 10.1002/ccta.2395
- [15] Bernacki, K., Rymarski, Z., Dyga, Ł. Selecting the coil core powder material for the output filter of a voltage source inverter. *Electronics Letters*, 2017, 53, 1068-1069. DOI: 10.1049/el.2017.1534
- [16] Matsumori, H., Shimizu, T., Wang, X., Blaabjerg, F. A Practical Core Loss Model for Filter Inductors of Power Electronic Converters. *IEEE Journal of Emerging and Selected Topics in Power Electronics*, 2018, 6, 29-39. DOI: 10.1109/JESTPE.2017.2761127
- [17] Shen, Y., Wang, H., Blaabjerg, F., Zhao H., Long, T. Thermal Modeling and Design Optimization of PCB Vias and Pads.

- IEEE Transactions on Power Electronics, 2020, (Early Access). DOI: 10.1109/TPEL.2019.2915029
- [18] Shringarpure, K., Pan, S., Kim, J., Fan, J., Achkir, B., Archambeault, B., Drewniak, J. Sensitivity Analysis of a Circuit Model for Power Distribution Network in a Multilayered Printed Circuit Board. IEEE Transactions on Electromagnetic Compatibility, 2017, 59, 1993-2001. DOI: 10.1109/TEMC.2017.2673851
- [19] Bernacki, K., Rymarski, Z. Electromagnetic compatibility of voltage source inverters for uninterruptible power supply system depending on the pulse-width modulation scheme. IET Power Electronics, 2015, 8, 1026-1034. DOI: 10.1049/iet-pel.2014.0637
- [20] Sharifzadeh, M., Vahedi, H., Portillo, R., Franquelo, L., Al-Haddad, K. Selective Harmonic Mitigation Based Self-Elimination of Triplen Harmonics for Single-Phase Five-Level Inverters. IEEE Transactions on Power Electronics, 2019, 34, 86-96. DOI: 10.1109/TPEL.2018.2812186
- [21] Saeedian, M., Adabi, M., Hosseini, S., Adabi, J., Pouresmae, E. A Novel Step-Up Single Source Multilevel Inverter: Topology, Operating Principle, and Modulation. IEEE Transactions on Power Electronics, 2019, 34, 3269-3282. DOI: 10.1109/TPEL.2018.2848359
- [22] Vahedi, H., Sharifzadeh, M., Al-Haddad, K. Modified Seven-Level Pack U-Cell Inverter for Photovoltaic Applications. IEEE Journal of Emerging and Selected Topics in Power Electronics, 2018, 6, 1508-1516. DOI: 10.1109/JESTPE.2018.2821663
- [23] IEEE Std 519-1992, IEEE Recommended Practices and Requirements for Harmonic Control in Electrical Power Systems, Second Printing 15 June 2004 DOI: 10.1109/IEEESTD.1993.114370
- [24] IEC 62040-3: 2011, Uninterruptible power systems (UPS) – Part 3: Method of specifying the performance and test requirements
- [25] Olhede, S., Walden, A. Generalized Morse wavelets. IEEE Transactions on Signal Processing, 2002, 50, 2661-2670. DOI: 10.1109/TSP.2002.804066
- [26] Lilly, J., Olhede, S. Higher-order properties of analytic wavelets. IEEE Transactions on Signal Processing, 2009, 57, 146-160. DOI: 10.1109/TSP.2008.2007607
- [27] Chikhalsouk, M., Zhou, K., El Okda, Y., Shinneeb, M. The applicability of the adaptive wavelet analysis in flutter identification in aerospace structures. In Proceedings of the 2018 Advances in Science and Engineering Technology International Conferences (ASET), Abu Dhabi, United Arab Emirates, 6 Feb – 5 April 2018, pp. 1-4. DOI: 10.1109/ICASET.2018.8376806
- [28] Mallat, S., Wavelet Tour of Signal Processing, 3rd ed.; Academic Press is an imprint of Elsevier 30 Corporate Drive, Suite 400 Burlington, MA, USA, 2009, DOI: 10.1016/B978-0-12-374370-1.X0001-8